Theory of the nuclear excitation by electron transition process near the *K* edge

E. V. Tkalya*

Institute of Nuclear Physics, Moscow State University, Ru-119992, Moscow, Vorob'evy Gory, Russia

(Received 12 September 2006; revised manuscript received 12 October 2006; published 21 February 2007)

We propose a model for description of the process of nuclear excitation by electron transition (NEET) near the *K*-shell ionization threshold of an atom. We explain the experimental results for the ^{197}Au excitation cross-section σ_N-obtained by Kishimoto *et al.* [Phys. Rev. C **74**, 031301(R) (2006)], using synchrotron radiation near the Au *K* edge. We predict the behavior of σ_N-as a function of the incident photon energy for the nuclei ^{193}Ir and ^{189}Os. We reveal that ^{189}Os excitation begins when the energy of incident photons is below the *K*-shell ionization threshold in Os.

DOI: 10.1103/PhysRevA.75.022509 PACS number(s): 32.30.Rj, 23.20.Nx, 27.70.+q, 27.80.+w

I. INTRODUCTION

Nuclear excitation by electron transition (NEET) [1] is a process of nonradiative nuclear excitation by means of direct energy transfer from the excited atomic shell to the nucleus via a virtual photon. This process is possible if within the atomic shell there exists an electronic transition close in energy and coinciding in type with the nuclear one.

The modern theory of NEET was developed in Refs. [2–7]. This theory agrees reasonably with experimental results obtained for the nuclei ^{197}Au [8], ^{193}Ir [9], and ^{189}Os [5] in recent years.

The NEET process was investigated in experiments [5,8,9] for the case where the energy of photons exceeded the *K*-shell electron binding energy appreciably. In such a situation one can neglect the threshold effects [2–4] and write the relative probability for nuclear excitation in an atomic transition, P_{NEET}, in the following form:

$$P_{NEET}=\left(1+\frac{\Gamma_i}{\Gamma_f}\right)\frac{E_{int}^2}{(\omega_N-\omega_A)^2+(\Gamma_i+\Gamma_f)^2/4}. \tag{1}$$

In Eq. (1) $\Gamma_{i,f}$ are the widths of the initial and final electronic states, ω_A and ω_N are the energies of the atomic and nuclear transitions (the adopted system of units is $\hbar=c=1$), and E_{int}^2 is averaged over the initial states and summed over the final ones, the square modulus of the Hamiltonian of the interaction H_{int} of the electronic hole current $j_{fi}^{\mu}(\mathbf{r})$ and the nuclear current $J_{fi}^{\nu}(\mathbf{R})$ in the second order of perturbation theory for quantum electrodynamics (QED),

$$H_{int}=\int d^3r\, d^3R\, j_{fi}^{\mu}(\mathbf{r})D_{\mu\nu}(\omega_N,\mathbf{r}-\mathbf{R})J_{fi}^{\nu}(\mathbf{R}), \tag{2}$$

where $D_{\mu\nu}(\omega_N,\mathbf{r}-\mathbf{R})$ is the photon propagator.

The cross section of ^{197}Au excitation on the isomeric level $1/2^+$ (77.351 keV, 1.91 ns) by photons near the *K*-shell ionization threshold of gold was measured in [10]. It was found that the NEET events occurred just above the *K* absorption edge and a NEET edge of width 14±9 eV existed at 40±2 eV higher than the *K* edge. The incident synchrotron radiation beam had a 3.5±0.1 eV width.

A theoretical explanation is needed for the results obtained in Ref. [10]. We consider here a model of the process found in Ref. [10] and describe the main characteristics of the process. Following the tradition we call this process "NEET near the *K* edge." However, here we pay attention to the cross section of the process of nuclear excitation as a result of ionization of the atomic *K* shell. NEET, as we shall see below, is a special case of the considered process in the asymptotic limit of "high" energies far from the photoionization threshold.

II. MODEL OF NEET PROCESS NEAR *K* EDGE

The process of nuclear excitation as a result of ionization of the atomic *K* shell is described by two diagrams shown in Fig. 1. One electron passes from the *K* shell to the continuum. We consider here the case of nuclear excitation by the atomic $M_I\rightarrow K$ transition.

According to the QED rules [11] the amplitude can be written as

$$S_{fi}^{(dir)}=-i\int d^4x_1d^4x_2d^4x_3\bar{\psi}_e(x_1)e\gamma^{\mu}A_{\mu}(x_1)G_h(x_1,x_2)\times e\gamma^{\nu}\psi_{h_{M_I}}(x_2)D_{\nu\rho}(x_2,x_3)J^{\rho}(x_3) \tag{3}$$

for the direct diagram [see Fig. 1(a)] and as

$$S_{fi}^{(ex)}=-i\int d^4x_1d^4x_2d^4x_3\bar{\psi}_e(x_1)\times e\gamma^{\mu}D_{\mu\rho}(x_1,x_3)G_h(x_1,x_2)e\gamma^{\nu}A_{\nu}(x_2)\psi_{h_{M_I}}(x_2)J^{\rho}(x_3) \tag{4}$$

for the exchange diagram [see Fig. 2(b)]. In Eqs. (3) and (4)

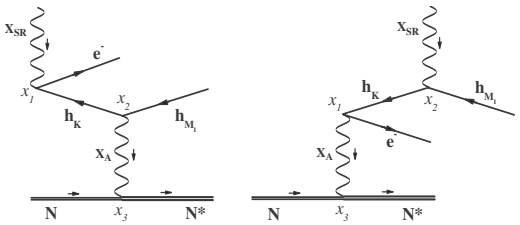

FIG. 1. Nuclear excitation by ionization of the atomic *K* shell: (a) direct diagram; (b) exchange diagram.

*Electronic address: tkalya@srd.sinp.msu.ru

e is the proton charge, γ^{μ} are the Dirac matrices. We will use the following designations for the wave functions of the particles and for the nuclear current shown in Fig. 1. $A_{\mu}(x;\omega_{SR})=e^{-i\omega_{SR}t}A_{\mu}(\mathbf{r};\omega_{SR})$ is the synchrotron radiation photon with energy ω_{SR}. $\bar{\psi}_e(x;E_e)=e^{iE_et}\bar{\psi}_e(\mathbf{r};E_e)$ is the electron with energy E_e emitted from the K shell to the continuum. $\psi_{h_{M_I}}(x;E_{M_I})=e^{-i(E_{M_I}-i\Gamma_{M_I}/2)t}\psi_{h_{M_I}}(\mathbf{r};E_{M_I})$ is the electron hole at the M_I shell with binding energy E_{M_I} and width Γ_{M_I}. The photon propagator $D_{\mu\nu}(x,x_3;\omega_N)=i\langle 0|\hat{T}A^{*}_{\mu}(x)A_{\nu}(x_3)|0\rangle$ is calculated according to the relation

$$D_{\mu\nu}(x,x_3;\omega_N)=\int\frac{d\omega}{2\pi}e^{i\omega_N(t-t_3)}D_{\mu\nu}(\mathbf{r}-\mathbf{R};\omega_N).$$

The nuclear current is $J^{\rho}(\mathbf{R},t_3)=e\Psi^{+}_{N^*}(\mathbf{R},t_3)\hat{J}^{\rho}\Psi_N(\mathbf{R},t_3)$, where the nuclear wave functions are $\Psi_N(\mathbf{R},t_3)=e^{-iE_Nt_3}\Psi_N(\mathbf{R})$ for the ground state ($E_N=0$ usually) and $\Psi^{+}_{N^*}(\mathbf{R},t_3)=e^{i(E_{N^*}+i\Gamma_{N^*}/2)t_3}\Psi^{+}_{N^*}(\mathbf{R})$ for the isomeric state with energy E_{N^*} and width Γ_{N^*}, and $\hat{J}^{\rho}$ is the operator of the nuclear electromagnetic transition. The propagator of the hole $G_h(x_1,x_2)=-i\langle 0|\hat{T}\psi_h(x_1)\bar{\psi}_h(x_2)|0\rangle$ in our model is the K-shell hole propagator

$$G_{h_K}(x_1,x_2;E_K)=-\psi_{h_K}(\mathbf{r}_1)\bar{\psi}_{h_K}(\mathbf{r}_2)\int\frac{dE}{2\pi}\frac{e^{iE(t_2-t_1)}}{E-E_K-i\Gamma_K/2},$$

where E_K is the electron binding energy and Γ_K is the total hole width at the K shell (see in Ref. [11]).

The model considered here has some peculiarities. Let us look at some of them more carefully. Let us begin from the NEET process. The excitation of the nuclei ^{197}Au, ^{193}Ir, and ^{189}Os takes place in reality in the electron transition from the M_I to the K shell, which occurs when a photon is absorbed and an electron in the K shell is excited into the continuum, leaving the K hole behind. The electrons in the atomic shell interact with each other and generate a self-consistent field providing that many-particle effects became very important for most of the processes inside the atomic shell. That is why one should take into account the ejected electron-hole interaction, the pair electron-electron interactions, etc., for correct description of the NEET process. Nevertheless, in our model the nucleus is excited in a single particle-hole transition, as shown on the diagrams in Fig. 1. Correspondingly we use the single-particle approximation for the calculation of the atomic matrix elements. One can do that, because numerous computations show that this approximation works well for electronic transitions between inner atomic shells, if one estimates the x-ray intensities, as well as for the electron transitions from inner atomic shells to the continuum, if one estimates the internal electronic conversion probabilities. That is why one can use this approximation to the numerical evaluation of the "electronic part" of the NEET.

We use the experimental values for the atomic shell widths. Therefore Γ_K in the propagators does not involve the NEET partial width. On the other hand the NEET probabilities are very small, and they do not change in practice the K-shell widths. For another thing we use the widths Γ_{M_I} for the final hole states on the diagrams in Fig. 1. This method is not typical for QED. As shown in Ref. [3], the use in the wave functions of the real widths of the vacancies enables us to take into account the further decay of the electron-hole into an upper atomic level without having to consider higher-order diagrams.

Another important approximation concerns the hole propagator. Strictly speaking all the atomic shells that have electrons contribute to the hole propagator. However, the energy conservation law leaves the K shell only in the hole propagator in the direct diagram in our case, because only one atomic transition (the $M_I\rightarrow K$ transition) satisfies the condition $\omega_A\simeq\omega_N$. The hole propagator in the exchange diagram may contain the contributions of all atomic shells. However, this propagator does not have poles in the discrete part of the spectrum; hence the contribution of the exchange diagram is negligible. As for the continuum spectrum there is no contribution of these hole states to the hole propagator in Fig. 1. A photon is absorbed by an electron in the atomic shell and a hole arises. The atomic inner hole state is a highly excited and short-lived discrete state. In the general case the wave function of the time-dependent state can be expressed as a decomposition into a sum and an integral over the complete set of eigenfunctions $\psi_{E_n}(\mathbf{x},t)$ with E_n belonging to the discrete spectrum ($E_n<0$), and $\psi_{\varepsilon}(\mathbf{x},t)$ with ε belonging to the continuous spectrum. Thus the propagator of the atomic inner hole generally should have two parts. But there are no electrons in the continuum in our case. The continuum is occupied by holes (i.e., by electron vacancies). These electron vacancies are fermions; hence hole creation is impossible in these states, and the transitions to these intermediate states are forbidden too. So these states do not give any contribution to the hole propagator at all. This becomes evident, if one considers the following process (which is identical to the one in Fig. 1): the hole in the continuum absorbs a photon and passes to the K shell first; after that the nucleus is excited in the hole transition $K\rightarrow M_I$. Only the atomic states occupied by electrons are "acting" intermediate states here, similarly to the process in Fig. 1. That is why we actually can neglect the continuum part of the energy spectrum in the hole propagator in Eqs. (3) and (4). As follows from comparison of the results of [2–6], the single-particle approximation describes well the NEET process with the simplest form of the propagator, and the technique of Feynman diagrams gives the same formula for the NEET probability that follows from solution of the equations for the time-dependent amplitudes of the total "hole+nucleus" wave function [5].

The cross section of the process shown in Fig. 1 is calculated from the following formula [11]:

$$\sigma_{N^*}=\int\frac{d^3p_e}{(2\pi)^3}\frac{\sum|S^{(dir)}_{fi}+S^{(ex)}_{fi}|^2}{T},$$

where Σ' means averaging over the initial states and summation over the final ones. The process progresses in the time interval T. We do not fix the electron energy E_e. That is why we integrate the cross section over the electron momentum p_e.

It is easy to show that after integration in Eqs. (3) and (4) over the times t_1,t_2,t_3 and over the energies of the intermediate states E,ω the amplitude $S_{fi}^{(ex)}$ contains only one resonance condition. This condition corresponds to the energy conservation law of the process. The amplitude $S_{fi}^{(dir)}$ has an additional resonance condition for the energy of photons $\omega_{SR}=E_e-E_K$. As a result the exchange diagram gives a contribution three orders of the magnitude smaller than the direct diagram. Correspondingly, one can neglect the exchange diagram Fig. 1(b) near the threshold. The following expression is obtained for the cross section in this case:

$$\sigma_{N^*}=\int \frac{d^3p_e}{(2\pi)^3}\frac{(2\pi)^2}{\Gamma_K}f(E_e)\frac{1}{2}\frac{1}{2J_N+1}\times\sum_{\lambda_{SR}}\sum_{m_e,m_{h_{M_I}}}\sum_{m_N,m_{N^*}}|H_{ion}|^2|H_{int}|^2. \quad (5)$$

In Eq. (5) we sum up over the photon polarization λ_{SR}, the magnetic quantum number of the free electron m_e, the magnetic quantum number of the M_I hole $m_{h_{M_I}}$, and the magnetic quantum numbers of the nucleus m_N,m_{N^*}. The function $f(E_e)$ is

$$f(E_e)=\frac{1}{\pi}\frac{\Gamma_K/2}{(\omega_{SR}-E_e+E_K)^2+\Gamma_K^2/4}\frac{1}{\pi}\times\frac{(\Gamma_{M_I}+\Gamma_{N^*})/2}{(\omega_{SR}-E_e+E_{M_I}-\omega_N)^2+(\Gamma_{M_I}+\Gamma_{N^*})^2/4}. \quad (6)$$

We introduced two new amplitudes H_{int} and H_{ion} in Eq. (5). The amplitude H_{int} describes an interaction between the electronic hole current $j_h^\nu(\mathbf{r}_2)=e\bar{\psi}_{h_K}(\mathbf{r}_2)\gamma^\nu\psi_{h_{M_I}}(\mathbf{r}_2)$ and the nuclear current $J^\rho(\mathbf{R})=e\Psi_{N^*}^+(\mathbf{R})\hat{J}^\rho\Psi_N(\mathbf{R})$ in the NEET process Eq. (2).

The expression Eq. (1) for the probability of nuclear excitation by the electron $i\to f$ $(M_I\to K)$ transition, P_{NEET}, can be adapted to the considered case of nuclear excitation by the electronic hole $K\to M_I$ transition by the replacement $\Gamma_{i,f}\to\Gamma_{M_I,K}$. The interaction energy E_{int} squared is, by definition, as follows:

$$E_{int}^2=\frac{1}{2j_{h_K}+1}\frac{1}{2J_N+1}\sum_{m_{h_K},m_{h_{M_I}}}\sum_{m_N,m_{N^*}}|H_{int}|^2.$$

It has the following form [4–6]:

$$E_{int}^2=4\pi e^2\omega_N^{2(L+1)}\frac{\left(j_i\frac{1}{2}L0\middle|j_f\frac{1}{2}\right)^2}{[(2L+1)!!]^2}|\mathcal{R}_L^{E/M}(\omega_N)|^2\times B(E/ML;J_i\to J_f), \quad (7)$$

where $B(E/(M)L;J_i\to J_f)$ is the nuclear reduced probability [12], and $\mathcal{R}_L^{E/(M)}$ are the atomic radial matrix elements of the electric (magnetic) $[E/M]$ multipolarity L [2–4], $\left(j_i\frac{1}{2}L0\middle|j_f\frac{1}{2}\right)$ is the Clebsch-Gordan coefficient, and $J_{i,f}$ and $j_{i,f}$ are the angular momenta of the nuclear and electronic states, respectively. It is obvious that the functions E_{int} and P_{NEET} do not depend on the energies ω_{SR} and E_e.

It should also be stated that we take $B(E/(M)L;J_i\to J_f)$ from the experimental data. We will consider below $M1$ transitions from the ground state to the first excited state in the nuclei ^{197}Au, ^{193}Ir, and ^{189}Os. $B(M1)$ for these transitions are known and can be taken form the tables [13–15]. As for the atomic $M1$ radial matrix elements they are calculated according to the formula [2–4]

$$\mathcal{R}_1^M(\omega)=(\kappa_i+\kappa_f)\int_0^\infty dr\,r^2h_1^{(1)}(\omega r)[g_i(r)f_f(r)+f_i(r)g_f(r)],$$

where $\kappa=(l-j)(2j+1)$, l is the orbital angular momentum, $h_L^{(1)}$ is the spherical Hankel function of the first kind [16], and $g(r)$ and $f(r)$ are, respectively, the large and small components of the electronic wave functions, with the condition of normalizing $\int_0^\infty dr\,r^2[g^2(r)+f^2(r)]=1$. Here these electron wave functions were evaluated by solving the relativistic Dirac-Fock equations in the self-consistent field of the electron shell taking into account the finite nuclear size. The computer program is described in detail in Ref. [17].

The amplitude H_{ion} corresponds to the process of the K-shell ionization by a photon

$$H_{ion}=-i\int d^3r_1e\bar{\psi}_e(\mathbf{r}_1)\gamma^\mu\psi_{h_K}(\mathbf{r}_1)A_\mu(\mathbf{r}_1;\omega_{SR}).$$

The cross section of the ionization process has the following form [11]:

$$d\sigma_{ion}=2\pi\delta(\omega_{SR}-E_e+E_K)\frac{1}{2}\sum_{\lambda_{SR}}\sum_{m_e,m_{h_K}}|H_{ion}|^2\frac{d^3p_e}{(2\pi)^3}, \quad (8)$$

where p_e is the electron momentum. Let us take into account that the expression $|H_{ion}|^2p_e\mathcal{E}_e$ $(\mathcal{E}_e=\sqrt{p_e^2+m^2}$, where m is the electron mass) depends little on the nonrelativistic kinetic energy of the electron, $E_e=p_e^2/2m$, near the threshold [11]. As a consequence we can introduce the following cross section near the threshold:

$$\sigma_{ion}^0=\lim_{p_e\to0}\int 2\pi\frac{1}{2}\sum_{\lambda_{SR}}\sum_{m_e,m_{h_K}}|H_{ion}|^2p_e\mathcal{E}_e\frac{d\Omega_e}{(2\pi)^3},$$

and we can consider σ_{ion}^0 as a constant in the energy range around the threshold.

The width of the K shell plays an important role in the process considered here. Let us "spread" out the δ function in Eq. (8) over the width Γ_K. The δ function is a limit of the δ-shaped Cauchy sequence. Therefore we can substitute $\delta(\omega_{SR}-E_e+E_K)\to(1/2\pi)\Gamma_K/[(\omega_{SR}-E_e+E_K)^2+\Gamma_K^2/4]$ in Eq. (8). Now if we compare the obtained expression with Eqs. (5) and (6) we get the following formula for the nuclear excitation cross section:

$$\sigma_{N^*}=\sigma_{ion}^0E_{int}^2\frac{2\pi}{\Gamma_K}\int_0^\infty f(E_e)dE_e. \quad (9)$$

When the incident photon energy ω_{SR} is near the K threshold, the function $f(E_e)$ in Eq. (6) decreases quickly when E_e increases in the range $0-(\Gamma_K+\Gamma_{M_I})$. That is why one can integrate in the range $0\leqslant E_e\leqslant\infty$ in Eq. (9) in spite of the fact that E_e is the nonrelativistic energy of the electron. The integral is calculated analytically:

$$\int_0^\infty f(E_e)dE_e = \frac{F_1 + F_2 + F_3}{[(\omega_N - \omega_A)^2 + (\Gamma_K + \Gamma_{M_I})^2/4][(\omega_N - \omega_A)^2 + (\Gamma_K - \Gamma_{M_I})^2/4]}, \tag{10}$$

where

$$F_1 = \frac{\Gamma_K}{2}\left((\omega_N - \omega_A)^2 + \frac{\Gamma_K^2 - \Gamma_{M_I}^2}{4}\right) \times \left[\frac{1}{2} + \frac{1}{\pi}\arctan\left(\frac{\omega_{SR} + E_{M_I} - \omega_N}{\Gamma_{M_I}/2}\right)\right],$$

$$F_2 = \frac{\Gamma_{M_I}}{2}\left((\omega_N - \omega_A)^2 - \frac{\Gamma_K^2 - \Gamma_{M_I}^2}{4}\right) \times \left[\frac{1}{2} + \frac{1}{\pi}\arctan\left(\frac{\omega_{SR} + E_{M_I} - \omega_A}{\Gamma_K/2}\right)\right],$$

$$F_3 = \frac{\Gamma_K}{2}\frac{\Gamma_{M_I}}{2}\frac{\omega_N - \omega_A}{\pi^2}\ln\left(\frac{(\omega_{SR} + E_{M_I} - \omega_A)^2 + (\Gamma_K/2)^2}{(\omega_{SR} + E_{M_I} - \omega_N)^2 + (\Gamma_{M_I}/2)^2}\right). \tag{11}$$

(We have neglected the nuclear level width because the following relation is true: $\Gamma_{N^*} \ll \Gamma_{M_I,K}$.) Formulas (9)–(11) give the cross section of nuclear excitation in the NEET process near the K-shell photoionization threshold for monochromatic photons. If the real synchrotron radiation (SR) beam has the width $\Delta\omega_{SR}$, one should integrate the cross section σ_{N^*} over the beam line shape: $\int g(\omega - \omega_{SR})\sigma_{N^*}(\omega)d\omega$. We used here the Gauss shape $g(\omega - \omega_{SR}) = (1/\sqrt{\pi}\Delta\omega_{SR})\exp\{-[(\omega - \omega_{SR})/\Delta\omega_{SR}]^2\}$. We will discuss some specific examples in Sec. III.

Let us see now how the cross section σ_{N^*} in Eq. (5) behaves in the range $\omega_{SR} \gg -E_K$, i.e., far from the photoionization threshold. Let us consider once more the expression for $f(E_e)$ in Eq. (6). The resonance ("δ-shaped") nature of the function $f(E_e)$ is evident for all values of ω_{SR}. The function $f(E_e)$ is different from zero in the range with the typical dimension $\Gamma_K + \Gamma_{M_I}$. The remaining functions under the integration sign in Eq. (5) change little in the mentioned range of E_e and can be taken outside the integral sign. As a result we can consider just the limiting value of the integral Eq. (10):

$$\lim_{\omega_{SR}\to\infty}\int_0^\infty f(E_e)dE_e = \frac{1}{2\pi}\frac{\Gamma_K + \Gamma_{M_I}}{(\omega_N - \omega_A)^2 + (\Gamma_K + \Gamma_{M_I})^2/4}. \tag{12}$$

If we substitute this result in Eq. (9) we obtain the following relation for the cross section far from the threshold:

$$\sigma_{N^*} = \sigma_{ion}P_{NEET}, \tag{13}$$

where the relative probability P_{NEET} was defined in Eq. (1). This result agrees well with the intuitive concept about factorization of the third-order graph in Fig. 1(a). That process can be represented as a succession of two processes in the incident photon energy range far from the threshold (where the threshold effects are not significant). The first process is an atomic shell photoionization, and the second process is, in fact, NEET. [It will be observed that the contribution of the exchange diagram in Fig. 1(b) decreases as $1/\omega_{SR}^2$ in the range $\omega_{SR} \gg -E_K$, i.e., this contribution is inessential as before.]

III. EXCITATION OF NUCLEI ^{197}Au, ^{193}Ir, AND ^{189}Os

Here we consider how the cross section looks for nuclei ^{197}Au, ^{193}Ir, and ^{189}Os near the K-shell ionization threshold. The functions $\sigma_{N^*}(\omega_{SR})/\sigma_{ion}^0 P_{NEET}$ are shown in Figs. 2–4 (i.e., all the cross sections σ_{N^*} in these figures are in units of $\sigma_{ion}^0 P_{NEET}$). We denote as Δ in Figs. 2–4 the difference between the energies of the nuclear and atomic transitions, $\Delta \equiv \omega_N - \omega_A$.

The following values of energies and widths were used for the cross section σ_{N^*} calculation of the nucleus ^{197}Au by formulas (9)–(11): $E_K = -80.725$ keV, $E_{M_I} = -3.425$ keV [18], $\Gamma_K = 52$ eV [19], $\Gamma_{M_I} = 14.3$ eV [19] (it should be noted that there are four various values for Γ_{M_I}, from 14.3 [19] to 20.9 eV [20], and here we use the value 14.3 eV recommended in the review [19]), $\omega_N = 77.351$ keV [13]. This nucleus is unique because the difference between the energies of the atomic transition ω_A and the nuclear transition ω_N is 50 eV only, i.e., this difference is commensurable with the atomic widths in the K and M_I shells of Au.

There are two kinds of line in Fig. 2. The solid lines correspond to excitation by a monochromatic beam. The dashed lines correspond to the real SR beam of Gaussian form with the width of 3.5 eV. It is evident from Fig. 2(a) that the nuclear excitation begins when the incident photon energy is above the threshold by 49 eV approximately. The effective width of the process [calculated with the function $d\sigma_{N^*}/d\omega_{SR}$, full width at half maximum (FWHM)] is close to the Γ_{M_I} width of Au for the monochromatic beam, and it is equal to 17–18 eV for the real SR beam. These results are in qualitative agreement with the experimental data [10].

There are two relatively small differences between the theoretical and experimental data for the NEET process in ^{197}Au at the present time. Experimentalists found that the NEET events occurred above the K absorption edge and a NEET edge of narrow width (=14±9 eV) existed at 40±2 eV higher than the K edge [10]. The theoretical values are approximately 19 and 49 eV, respectively. The NEET probability P_{NEET} measured in [10] was $(4.5\pm0.6)\times10^{-8}$, whereas the theoretical value calculated by Eqs. (1) and (7) is $(3.4\pm0.2)\times10^{-8}$ with the nuclear reduced probability in Weisskopf units $B_{W.u.}(M1; 1/2^+ \to 3/2^+) = (2.05\pm0.08)$

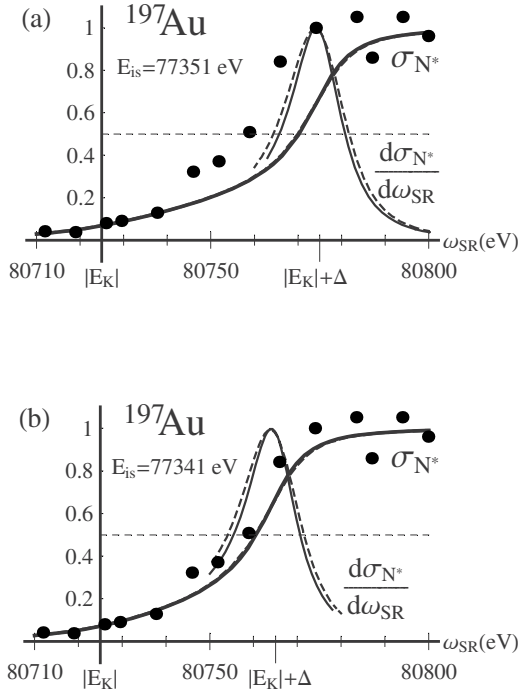

FIG. 2. Excitation cross section of the nucleus ^{197}Au in units of $\sigma^0_{ion}P_{NEET}$ ($\simeq 1.3\times10^{-28}$ cm^2). Solid lines, excitation by a monochromatic beam; dashed lines, excitation by the synchrotron radiation beam with 3.5 eV width. Closed circles are the experimental data from Ref. [10], Fig. 3(b). (a) The energy of the isomeric level E_{is}=77.351 keV and $\Delta=\omega_N-\omega_A$=51 eV; (b) E_{is}=77.341 keV and Δ=41 eV.

$\times10^{-3}$ [13] and the atomic matrix element evaluated here $|\mathcal{R}^M_1(\omega_N;M_I\rightarrow K)|^2$=106.8. It is interesting to note that the mentioned differences can be removed. The energy of the isomeric level E_{is} in ^{197}Au is 77.351 keV [13]. Kishimoto suggested considering another value for the energy of the nuclear transition, viz., 10 eV less than the tabulated value [21]. When using the value E_{is}=77.341 keV in theoretical calculations, one obtains 40 eV delay and 17.5 eV width for the NEET process near the K edge [see Fig. 2(b)], and $P_{NEET}=(4.5\pm0.2)\times10^{-8}$ far from the K edge. [We neglected here the error bar for $|\mathcal{R}^M_1(\omega_N;M_I\rightarrow K)|^2$, because the atomic matrix elements are evaluated usually with an accuracy of 0.1% for the transitions between inner shells.] Such a good agreement with the available experimental data points to the

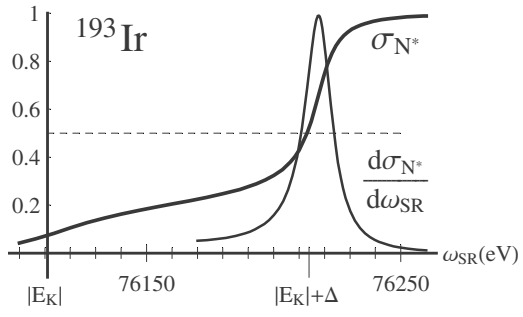

FIG. 3. Excitation cross section of ^{193}Ir in units of $\sigma^0_{ion}P_{NEET}$ ($\simeq6.6\times10^{-30}$ cm^2), Δ=107 eV.

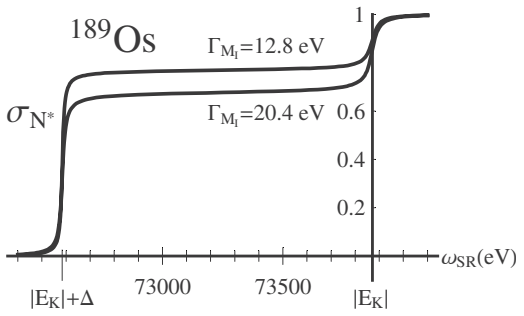

FIG. 4. Excitation of ^{189}Os below the K-shell ionization threshold for two Γ_{M_I} width values. σ_{N^*} is in units of $\sigma^0_{ion}P_{NEET}$ ($\simeq4\times10^{-31}$ cm^2), Δ=−1287 eV.

necessity of making a more precise measurement of the energy of the first excited state in ^{197}Au. In conclusion, the value $\sigma^0_{ion}P_{NEET}\simeq1.3\times10^{-28}$ cm^2 presented in Fig. 2 was obtained with the experimental value $P_{NEET}=4.5\times10^{-8}$ [10] and the tabulated ionization cross section near the K edge of Au $\sigma^0_{ion}=2.85\times10^{-23}$ cm^2 [22].

The nuclear excitation cross section on ^{193}Ir is shown in Fig. 3. We used the following values of energies and widths [18,19] for the calculation of the cross section: E_K =−76.111 keV, E_{M_I}=−3.174 keV, Γ_K=45 eV, Γ_{M_I} =12.8 eV, and ω_N=73.04 keV [14]. Calculation of $\sigma^0_{ion}P_{NEET}$ gives the result $\sigma^0_{ion}P_{NEET}\simeq6.6\times10^{-30}$ cm^2. We used σ^0_{ion} $=3.28\times10^{-23}$ cm^2 from Ref. [22] and $P_{NEET}=2.0\times10^{-9}$ evaluated with $B_{W.u.}(M1;1/2^+\rightarrow3/2^+)=4.9\times10^{-4}$ [14], and $|\mathcal{R}^M_1(\omega_N;M_I\rightarrow K)|^2$=105.3. The excitation of the nucleus begins when the incident photon energy is above the threshold—$\omega_{SR}=-E_K+\omega_N-\omega_A$. The effective width of the process is close to the Γ_{M_I} width of Ir.

In ^{189}Os the atomic transition energy $\omega_A=E_{M_I}-E_K$ =70.822 keV [18] exceeds the energy of the nuclear transition ω_N=69.535 keV [15] in contrast to ^{197}Au and ^{193}Ir. Furthermore, the difference $\omega_A-\omega_N$=1287 eV considerably exceeds the atomic width values Γ_K=42.6 eV [19], Γ_{M_I} =20.4 eV [20]. The nuclear excitation cross section is shown in Fig. 4. We see that the excitation of the nucleus begins when the incident photon energy is below the K-shell ionization threshold: $\omega_{SR}=-E_K-1.287$ keV. The lower line in Fig. 4 corresponds to the width Γ_{M_I}=20.4 eV from Ref. [20]; the upper line corresponds to the width Γ_{M_I}=12.8 eV (this value is an approximation obtained from the data in Ref. [19]). The

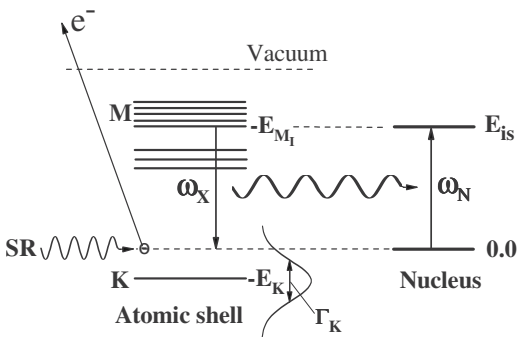

FIG. 5. Diagram of the subthreshold excitation of a nucleus.

value of σ_N averages 0.7–0.8 in units of $\sigma^0_{ion}P_{NEET}$ in the range $-E_K-(\omega_A-\omega_N)\leqslant\omega_{SR}\leqslant-E_K$. It means that the SR photons effectively excite the nucleus below the ionization threshold.

As regards the numerical value $\sigma^0_{ion}P_{NEET}\simeq 4\times10^{-31}$ cm^2 in Fig. 4, it was obtained with $P_{NEET}=1.2\times10^{-10}$ [2] and the tabulated ionization cross section near the K edge of Os, $\sigma^0_{ion}=3.4\times10^{-23}$ cm^2 [22].

Subthreshold excitation is a quantum effect. The K-shell vacancy has a sizable width. As a consequence, incident photons with energy below the binding energy $-E_K$ can ionize the K shell. In this case the energy of the emitted photon in the electron $M_1\rightarrow$K transition satisfies the condition $\omega_X<E_{M_1}-E_K$ (see Fig. 5). On the other hand the energy of the nuclear transition in ^{189}Os satisfies the analogous condition $\omega_N<\omega_A\equiv E_{M_1}-E_K$. That is why the nuclear subthreshold excitation is possible. This very effect is observed in Fig. 4.

The K-shell hole is an intermediate state in such a process, and the parameters of this state are not included into the energy conservation law $(1/2\pi)\Gamma_{M_1}/[(\omega_{SR}-E_e+E_{M_1}-\omega_N)^2+\Gamma^2_{M_1}/4]$, which is an analog of the typical δ function $\delta(\omega_{SR}-E_e+E_{M_1}-\omega_N)$ connecting the initial and final states in Fig. 1. Therefore, the energy range where there occurs the first ("basic") resonance growth of the cross section of the ^{189}Os nucleus excitation (the area of the left "step" in Fig. 4) is equal to Γ_{M_1}. For the same reason at the interval with the width of Γ_{M_1}, but beyond the ionization threshold, there also occurs the growth of the ^{193}Ir excitation. In ^{197}Au the width of the excitation cross section is a bit greater than Γ_{M_1}. The difference between the energies of atomic and nuclear transitions in ^{197}Au is about the width of the vacancy for the K shell of Au. As a result, the second resonance at $\omega_{SR}=-E_K$ has an influence on the width of the excitation cross section at $\omega_{SR}=-E_K+(\omega_N-\omega_A)$ and makes this basic resonance somewhat broader. [We used the appellation "basic," because in the case of a wide interval between the resonances the amplitude of the resonance at $\omega_{SR}=-E_K$ is smaller by a factor of Γ_K/Γ_{M_1} approximately than the amplitude of the basic resonance at $\omega_{SR}=-E_K+(\omega_N-\omega_A)$.]

IV. CONCLUSION

Finally, it should be noted that studying the processes of interaction between a nucleus and an atom shell is quite a topical task. One of the reasons is an active search, especially in recent years, for acceleration mechanisms for isomeric state decay of nuclei by an external influence upon the atomic shell. A number of attempts of this type were analyzed in [23]. NEET and other similar processes become most important in this case. The perturbation theory for QED can best of all be used to systematize and to well fit the mentioned phenomena, and the present work is another confirmation of this view. The theory of NEET developed within the framework of perturbation theory for QED gives results that are in agreement with experimental data both qualitatively and quantitatively in a wide range of energy including the range of ionization thresholds of atoms.

ACKNOWLEDGMENT

I thank Professor S. Kishimoto for providing me with the experimental data and for a useful discussion on the NEET mechanism.

[1] M. Morita, Prog. Theor. Phys. **49**, 1574 (1973).
[2] E. V. Tkalya, Nucl. Phys. A **539**, 209 (1992).
[3] E. V. Tkalya, Zh. Eksp. Teor. Fiz. **102**, 379 (1992). , [Sov. Phys. JETP **75**, 200 (1992)].
[4] E. V. Tkalya, in *X-ray and Inner-Shell Processes*, edited by R. W. Dunford, D. S. Gemmell, E. P. Kanter, B. Krässig, S. H. Southworth, and L. Young, AIP Conf. Proc. No. 506 (AIP, Melville, NY, 2000), p. 486.
[5] I. Ahmad *et al.*, Phys. Rev. C **61**, 051304(R) (2000).
[6] M. R. Harston, Nucl. Phys. A **690**, 447 (2001).
[7] E. V. Tkalya, Zh. Eksp. Teor. Fiz. **105**, 449 (1994). [JETP **78**, 239 (1994)].
[8] S. Kishimoto *et al.*, Phys. Rev. Lett. **85**, 1831 (2000).
[9] S. Kishimoto *et al.*, Nucl. Phys. A **748**, 3 (2005).
[10] S. Kishimoto *et al.*, Phys. Rev. C **74**, 031301(R) (2006).
[11] V. B. Berestetskii, E. M. Lifschitz, and L. P. Pitaevskii, *Quantum Electrodynamics* (Pergamon Press, Oxford, 1982).
[12] A. Bohr and B. Mottelson, *Nuclear Structure. Vol. 1. Single-Particle Motion* (W.A. Benjamin, New York, 1969).
[13] H. Xiaolong and Z. Chunmei, Nucl. Data Sheets **104**, 283 (2005).
[14] A. Artna-Cohen, Nucl. Data Sheets **83**, 921 (1998).
[15] S. C. Wu and H. Niu, Nucl. Data Sheets **100**, 1 (2003).
[16] *Handbook of Mathematical Functions*, Natt. Bur. Stand. Appl. Math. Ser. No. 55, edited by M. Abramowitz and I. A. Stegun (U.S. GPO, Washington, D. C., 1969).
[17] I. M. Band and V. I. Fomichev, At. Data Nucl. Data Tables **23**, 295 (1979).
[18] NIST Physical Reference Data, http://physics.nist.gov/PhysRefData/contents.html.
[19] J. L. Campbell and T. Papp, At. Data Nucl. Data Tables **77**, 1 (2001).
[20] E. J. McGuire, Phys. Rev. A **5**, 1043 (1972).
[21] S. Kishimoto (private communication).
[22] W. Veigele, At. Data **5**, 1 (1973).
[23] E. V. Tkalya, Usp. Fiz. Nauk **175**, 555 (2005) [Phys. Usp. **48**, 525 (2005)].